IMPACT CRATER MAXIMUM DEPTH OF PENETRATION AND EXCAVATION; John D. O'Keefe and Thomas J. Ahrens, Seismological Laboratory 252-21, California Institute of Technology, Pasadena, California 91125.

Using a finite difference computer model to solve the material response field equations (Thompson, 1979) we addressed the issues of: 1) What is the maximum depth that the impactor penetrates a planetary surface?, and 2) What is the maximum depth that is excavated by the cratering flow? We calculated the flow fields from the impact of a projectile having a dimensionless radius of ga/U^2, where the impact velocity, U= 12 km/s and the gravitational acceleration, g, ranged from 1 to 10^6 times the Earth's. This allowed us to study the effects of varying either the radius of the impactor, a, at a fixed gravity or the gravitational acceleration at a fixed impactor radius. As an example, for the Earth's gravitational acceleration, the projectile radius, a, varied from 5 m to 5×10^6 m. The planetary strength was varied from nominal values to zero for hydrodynamic flows. The deformations in the planetary surface and the trajectories of the material in the planet were delineated by the use of massless tracer particles.

For dimensionless times $(Ut/a) < 5$, the crater depth increased linearly with time (Fig. 1). The exceptions were for values of $ga/U^2 > 10^{-2}$ (e.g. a > 50 km for Earth impacts). For $(Ut/a) > 5$, but less than the rebound time, the craters grew at a slower rate. This rate is consistent with that predicted by Holsapple and Schmidt (1987) from dimensional considerations and the introduction of the concept of a coupling coefficient. At large values of ga/U^2 ($> 10^{-2}$) and relative strength, $Y/U^2\rho > 10^{-2}$, the gravitational or deformation work are significant during initial penetration and the conditions for the validity of the coupling coefficient are violated.

We determined the maximum depth of penetration and excavation as a function of crater radius for impacts on the Earth, Mars, and the Moon at 12 km/sec (Fig. 2). The depth of excavation increases relative to the crater radius, r, because the crater radius decreases relative to impacting body radius with the increasing size. For example, these curves predict that a 100 km diameter crater on the Earth would have ejected material from a depth of only $\sim$ 23 km.

Massless tracer particles were placed in planes below the point of impact and were used to determine the deformations and trajectories of particles relative to their initial positions in the planet. The deformations and particle trajectories were essentially identical for: 1) times up to the point of maximum depth of penetration, 2) a given value of strength, and 3) for $ga/U^2 < 10^{-2}$ (e.g. radii $\gtrsim$ 50 km for g = 980 cm/s^2). An example of the particle trajectories and the velocity field for a case that corresponds to a 50 km radius impactor on the Earth is shown in figure 3. Referring to the trajectories, note that for the positions under the point of impact, and for a range of angles $< 10^\circ$, that the flow is nearly radially outward. At angles greater than this, the flow field is no longer purely radial, it has the downward and then upward motion as assumed in the Z-model (Maxwell, 1977). At late times, because of the influence of gravity, the velocity field has a toroidal geometry that gives rise to the rebounding of the crater floor. The turning around and hooking of the trajectories chronicles that behavior. The rebounding occurs at a dimensionless time of $\sim$ 20 , (for $ga/U^2 < 10^{-2}$). The deformational histories of annular columns of material beneath the planetary surface are also shown in figure 4. Note that the columnar structure near the impact centerline is nearly a reconstruction of the structure at an earlier time. This behavior has been a source of debate in the interpretation of experiments at high accelerations in centrifuge experiments (Schmidt and Holsapple, 1981). We now conclude that at high accelerations, or at large scales, that a deep transient bowl-shaped crater is always produced. However, subsequent rebounding motions produce the observed shallow final crater. The relative depth of excavation d_e/r of Fig. 1 for earth gravity and impact at 12 km/sec yields in (cgs, units) $d_e/r = 0.02r^{0.20}$. Thus the maximum depth of penetration and excavation increase slowly with crater radius.

References: **(1)** Holsapple, K. A. and R. M. Schmidt (1987), Point-source solutions and coupling parameters in cratering mechanics, *J. Geophys. Res.*, in press. **(2)** Maxwell, D. E. (1977), Simple Z model cratering, ejection, and the overturned flap, *Proc. Symp. Impact and Explosion Cratering*, ed. by D. J. Roddy, R. O. Pepin, and R. B. Merrill, Pergamon, 1003-1008. **(3)** Schmidt, R. M. and K. R. Hansen (1986), Gravity-regime scaling for impact crater size in non-porous targets, *abstract, EOS, 67*, 1078-1079. **(4)** Schmidt, R. M. and K. A. Holsapple (1981), An experimental investigation of transient crater size, *Lunar & Planet. Science XII*, 934-936. **(5)** Thompson, S. L. (1979), CSQI Eulerian finite difference program for two-dimensional material response, SAND 77-1339, Sandia National Labs, Albuquerque, N.M.

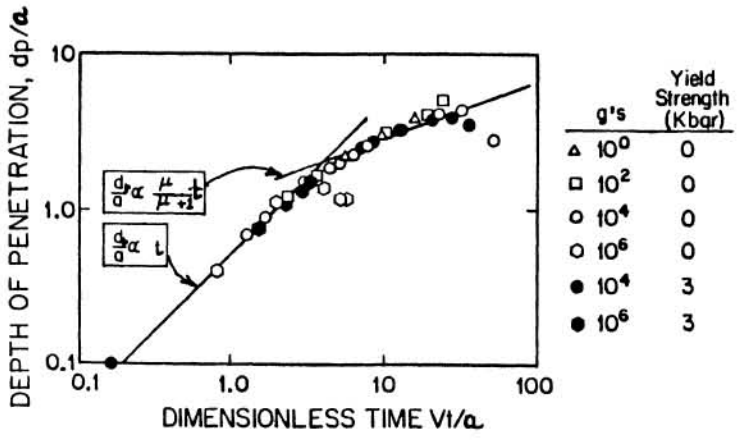

Fig. 1. Relative depth of penetration of impact crater produced in silicate at 12 km/sec, versus non-dimensional time. Points for various Tresca yield strength targets are indicated.

IMPACT CRATER DEPTH
O'Keefe, J. D. and Ahrens, T. J.

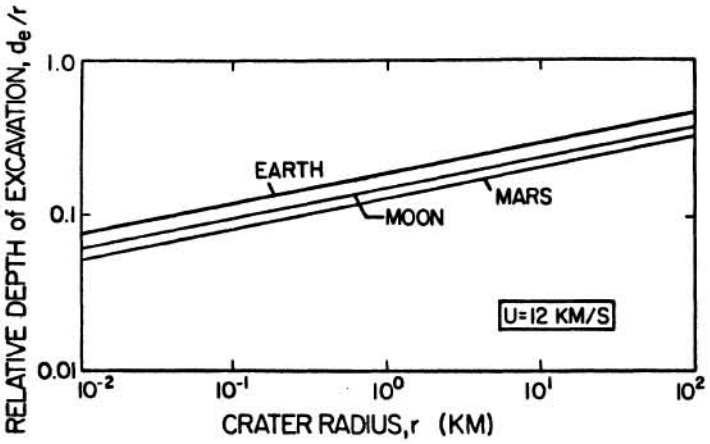

Fig. 2. Maximum depth of excavation normalized by crater radius, versus crater radius for Earth, Moon, and Mars for 12 km/sec impact of silicate projectile impacting silicate half-space.

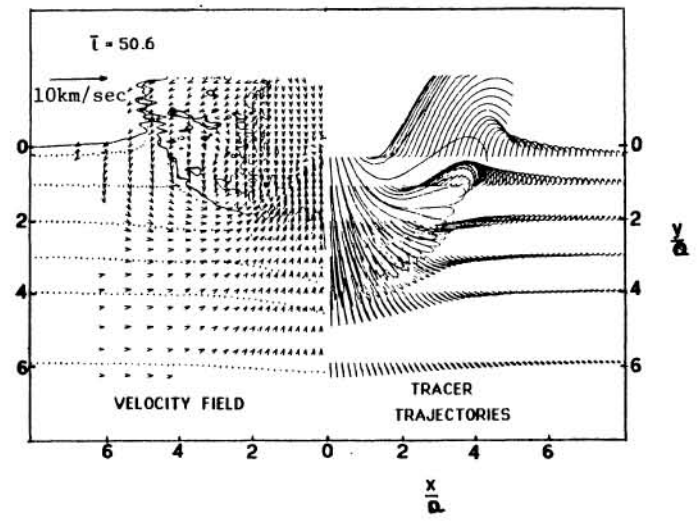

Fig. 3. Velocity field resulting from 50 km silicate projectile impacting at 12 km/sec, onto a silicate half-space at the dimensionless time, $\bar{t}$ = 50.6 and the massless tracer particle histories up to that time.

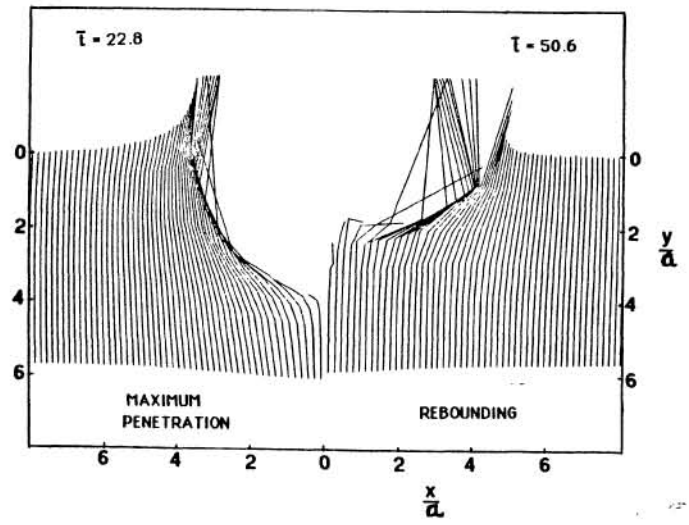

Fig. 4. Vertical columnar markers showing the planetary surface deformations at the time of maximum penetration ($\bar{t}$ = 22.8) and during the rebounding of the crater floor ($\bar{t}$ = 50.8). The impact conditions are the same as in fig. 3.